Statistical mechanics of dense granular media

2005 J. Phys.: Condens. Matter 17 S2557

(http://iopscience.iop.org/0953-8984/17/24/013)

INSTITUTE OF PHYSICS PUBLISHING JOURNAL OF PHYSICS: CONDENSED MATTER

J. Phys.: Condens. Matter **17** (2005) S2557–S2572 doi:10.1088/0953-8984/17/24/013

Statistical mechanics of dense granular media

A Coniglio, A Fierro, M Nicodemi, M Pica Ciamarra and M Tarzia

Dipartimento di Fisica, Università di Napoli 'Federico II', INFM, Unità di Napoli, Complesso Universitario Monte Sant'Angelo, Via Cinthia, I-80126, Napoli, Italy

Received 16 March 2005
Published 3 June 2005
Online at stacks.iop.org/JPhysCM/17/S2557

Abstract

We discuss some recent results on the statistical mechanics approach to dense granular media. In particular, by analytical mean field investigation we derive the phase diagram of monodisperse and bidisperse granular assemblies. We show that 'jamming' corresponds to a phase transition from a 'fluid' to a 'glassy' phase, observed when crystallization is avoided. The nature of such a 'glassy' phase turns out to be the same as found in mean field models for glass formers. This gives quantitative evidence for the idea of a unified description of the 'jamming' transition in granular media and thermal systems, such as glasses. We also discuss mixing/segregation transitions in binary mixtures and their connections to phase separation and 'geometric' effects.

(Some figures in this article are in colour only in the electronic version)

1. Introduction

An important conceptual open problem concerning granular media is the absence of an established theoretical framework where they might be described. Several methods and theories, many of them reviewed in this volume, have been put forward in recent years. Edwards [1, 2], in particular, proposed first that a statistical mechanics approach might be feasible to describe dense granular media. He introduced the hypothesis that time averages of a system, exploring its mechanically stable states subject to some external drive (e.g., 'tapping'), coincide with suitable ensemble averages over its 'jammed states'.

The statistical mechanics approach to dense granular media was later supported by observations from experiments [5, 7] and simulations [13, 11] which suggested that when the system approaches stationarity during its 'tapping' dynamics, its macroscopic properties are univocally characterized by a few control parameters and do not depend on the system initial configuration or dynamical protocol. Of course, the open problem remains to understand and predict the features of the 'suitable' ensemble average for the system. This is a very important current research issue in granular media which has recently seen interesting contributions from both computer simulations and experiments.

We discuss here the basic ideas in the statistical mechanics of dense granular media at stationarity and recent results about its extensions. A central concept in this approach is the configurational entropy, $S_{\rm conf} = \ln \Omega$, where $\Omega(E, V)$ is the number of mechanically stable states corresponding to the volume V and energy E. From $S_{\rm conf}$ conjugated thermodynamic parameters can be derived: the compactivity, $X^{-1} = \partial S_{\rm conf}/\partial V$, and the configurational temperature $T_{\rm conf}^{-1} = \partial S_{\rm conf}/\partial E$. The 'thermodynamic' parameters should completely characterize the macroscopic properties of the system, as much as pressure or ordinary temperatures in gases. Methods have been developed, thus, to measure these parameters by exploiting different techniques. In the stationary regime we consider here, for instance, one can show that $T_{\rm conf}$ can be related to an *equilibrium* fluctuation–dissipation (FD) theorem [28, 29, 11, 30, 31]. As reviewed in section 2, this allows a simple evaluation of $T_{\rm conf}$ from measures, for example, of the sample bulk density (or height) and its fluctuations, taken in the stationary regime of, e.g., a tap dynamics. The knowledge of the system distribution function and its parameters can be exploited to depict a first theoretical comprehensive picture of the vast phenomenology of powders, ranging from their phase diagrams to segregation properties. This was partially accomplished in [11, 34, 36].

A different approach [25, 26, 13] to measure an 'effective temperature', $T_{\rm dyn}$, in granular media which are far from stationarity is based on the *out-of-equilibrium* extension of the fluctuation–dissipation theorem discovered in glassy theory [23, 22]. Interestingly, it was shown [26, 13, 31] that in the limit of small shaking amplitudes $T_{\rm dyn}$ coincides with the above 'configurational temperature', $T_{\rm conf}$.

We review below the basic ideas in the statistical mechanics of dense monodisperse granular media at stationarity and in such a framework derive their 'phase diagram' in the mean field approximation. This allows us to discuss the nature of jamming in non-thermal systems [9, 10] and the origin of its close connections to glassy phenomena in thermal ones [2]. As an extension and a further application of this approach, we also consider the intriguing phenomenon of segregation in bidisperse mixtures.

2. Statistical mechanics of dense granular media

In this section we summarize the essential ideas in the statistical mechanics of dense granular media [4, 2]. These are strongly dissipative systems not affected by temperature, because thermal fluctuations are usually negligible. Therefore, in the absence of driving, the usual temperature of the external bath can be considered zero and these media called *non-thermal*. As the system cannot explore its phase space (unless perturbed by external forces, such as shaking or tapping) it is frozen, at rest, in its mechanically stable microstates (see figure 1).

In the statistical mechanics of powders introduced by Edwards [1] it is postulated that the system at rest (i.e., not in the 'fluidized' regime) can be described by suitable ensemble averages over its 'mechanically stable' states. The issue is to individuate the probability, P_r, to find the system in its generic mechanically stable state r. A possible approach to find P_r stems [11] from the maximization of the system entropy,

$$S = -\sum_r P_r \ln P_r \tag{1}$$

with the macroscopic constraint, in the case of the canonical ensemble, that the system average energy, $E = \sum_r P_r E_r$, is given. This assumption leads to the Gibbs result:

$$P_r \propto \mathrm{e}^{-\beta_{\rm conf} E_r} \tag{2}$$

where $\beta_{\rm conf}$ is a *Lagrange multiplier*, called the *inverse configurational temperature*, enforcing

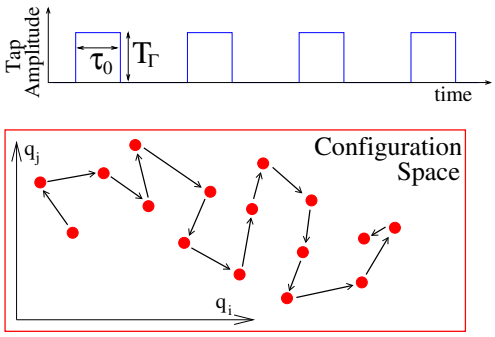

Figure 1. The present models for granular media are subject to a Monte Carlo dynamics made up of 'tap' sequences. A 'tap' is a period of time, of length τ_0 (the tap duration), during which the system evolves at a finite bath temperature T_Γ (the tap amplitude); after each 'tap' the system evolves at $T_\Gamma = 0$ and reaches a mechanically stable state in its exploration of the configuration space.

the above constraint on the energy:

$$\beta_{\rm conf} = \frac{\partial S_{\rm conf}}{\partial E} \qquad S_{\rm conf} = \ln \Omega(E). \tag{3}$$

Here, $\Omega(E)$ is the number of mechanically stable states with energy E. Thus, summarizing, the system at rest has $T_{\rm bath} = 0$ and $T_{\rm conf} = \beta_{\rm conf}^{-1} \neq 0$. Analogously, by assuming that the system volume, V, is given (as in Edwards' original approach [1, 2]), similar calculations lead to $P_r \propto {\rm e}^{-V_r/\lambda X}$, where V_r is the volume of microstate r and $X = \lambda^{-1}(\partial S_{\rm conf}/\partial V)^{-1}$ is called the compactivity.

These basic considerations, to be validated by experiments or simulations, settle a theoretical statistical mechanics framework to describe granular media. Consider, for definiteness, a system of monodisperse hard spheres of mass m. In the whole configuration space $\Omega_{\rm Tot}$ of the system, we can write Edwards' generalized partition function as

$$Z = \sum_{r \in \Omega_{\rm Tot}} \exp(-\mathcal{H}_{\rm HC} - \beta_{\rm conf} mgH) \cdot \Pi_r \tag{4}$$

where $\mathcal{H}_{\rm HC}$ is the hard-core interaction between grains, mgH is the gravity contribution to the energy (H is particle height), and the factor Π_r is a projector on the space of 'mechanically stable' states Ω: if $r \in \Omega$ then $\Pi_r = 1$ else $\Pi_r = 0$.

As well as in usual equilibrium 'thermal' statistical mechanics, it is straightforward to verify that in the present approach a 'standard' (i.e., not 'out-of-equilibrium') fluctuation–dissipation (FD) theorem holds, linking at stationarity, for instance, the system average energy, E, to its fluctuations, ΔE^2:

$$-\frac{\partial E}{\partial \beta_{\rm conf}} = \Delta E^2. \tag{5}$$

Usefully, the integration of such an *equilibrium* FD relation may provide direct access to $\beta_{\rm conf}$ from energy (or density, etc) data measured at stationarity [11]:

$$\beta_{\rm conf}(E) = \beta_{\rm conf}^0 - \int_{E_0}^{E} (\Delta E^2)^{-1} \, {\rm d}E. \tag{6}$$

Summarizing, such an 'equilibrium' statistical mechanics approach is based on the hypothesis that at stationarity the system properties do not depend on the details of the dynamical history. This has to be checked by computer simulations and experiments. The

next step is to verify that a few macroscopic parameters (such as energy or density, etc) are completely characterizing the status of the system, i.e., that a 'thermodynamic' description is indeed possible. In such a case, $\beta_{\rm conf}$ can be derived, for example, from equation (6). Finally, one must check that time averages obtained using such a dynamics compare well with ensemble averages over the distribution equation (2).

In the following sections we discuss some recent results [27, 11] about schematic models validating and generalizing Edwards' statistical mechanics approach. In particular, we show by mean field analytical calculations that granular media undergo a phase transition from a (supercooled) 'fluid' phase to a 'glassy' phase, when their crystallization transition is avoided. The nature of such a 'glassy' phase turns out to be the same as found in mean field models for glass formers: a discontinuous one-step replica symmetry breaking phase preceded by a dynamical freezing point. These results are supported by Monte Carlo (MC) 'tap dynamics' simulations which, in the region of low MC shaking amplitudes, show a pronounced jamming similar to the one found in experiments on granular media. As an application to mixtures we also discuss segregation/mixing phenomena in these systems.

3. Hard sphere schematic models for granular media

The simplest model for granular media we considered [11] is a monodisperse system of hard spheres of equal diameter $a_0 = 1$, subjected to gravity. In order to check the above statistical mechanics scenario, we consider now a simplified version of such a model, where we constrain the centres of mass of the spheres to move on the sites of a cubic lattice (see inset in figure 3). The Hamiltonian of the system is

$$\mathcal{H} = \mathcal{H}_{\rm HC}(\{n_i\}) + gm \sum_i n_i z_i, \tag{7}$$

where the height of site i is z_i, $g = 1$ is the gravity acceleration, $m = 1$ the grain mass, $n_i = 0, 1$ the usual occupancy variable (i.e., $n_i = 0$ or 1 if site i is empty or filled by a grain) and $\mathcal{H}_{\rm HC}(\{n_i\})$ a hard-core interaction term that prevents the overlapping of nearest-neighbour grains (this term can be written as $\mathcal{H}_{\rm HC}(\{n_i\}) = J \sum_{\langle ij \rangle} n_i n_j$, where the limit $J \to \infty$ is taken).

The grains are subject to a dynamics made up of a sequence of Monte Carlo 'taps' (see figure 1): a single 'tap' [8] is a period of time, of length τ_0 (the tap duration), where particles can diffuse laterally, upwards with probability $p_{\rm up} \in [0, 1/2]$, and downwards with probability $1 - p_{\rm up}$. When the 'tap' is off grains can only move downwards (i.e., $p_{\rm up} = 0$) and the system evolves with $p_{\rm up} = 0$ until it reaches a blocked configuration (i.e., an 'inherent state') where no grain can move downwards without violating the hard-core repulsion. The parameter $p_{\rm up}$ has an effect equivalent to keeping the system in contact (for a time τ_0) with a bath temperature $T_\Gamma = mga_0/\ln[(1 - p_{\rm up})/p_{\rm up}]$ (called the 'tap amplitude'). The properties of the system are measured when this is in a blocked state. Time averages, therefore, are averages over the blocked configurations reached with this dynamics. Time t is measured as the number of taps applied to the system.

Under such a tap dynamics the systems reaches a stationary state where the statistical mechanics approach to granular media can be tested, and particularly the Edwards hypothesis can be verified by comparing time averages to ensemble averages of equation (2).

3.1. Stationary states and time averages

During the tap dynamics, in the stationary state, the time average of the energy, $\overline{E}$, and its fluctuations, $\overline{\Delta E^2}$, are calculated.

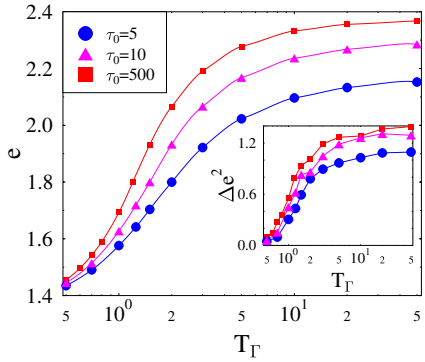

Figure 2. The time average of the energy, $e = \overline{E}$, and (inset) its fluctuations, $\Delta e^2 = \overline{\Delta E}^2$, recorded at stationarity during tap dynamics, as a function of the tap amplitude, T_Γ, in the 3D lattice monodisperse hard-sphere model. Different curves correspond to sequences of taps with different values of the duration of each single tap, τ_0.

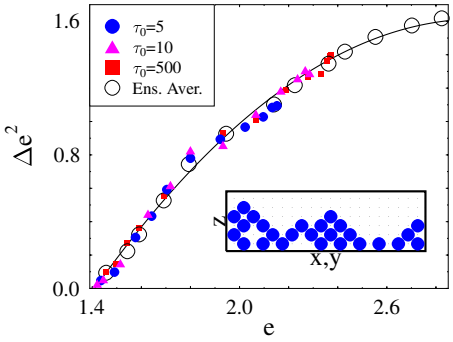

Figure 3. Energy fluctuations Δe^2 plotted as a function of the energy e. The symbols ●, ▲ and ■ are time averages, $\overline{E}$ and $\overline{\Delta E}^2$, obtained with different tap dynamics in figure 2. The symbols ○ are independently calculated ensemble averages, $\langle E \rangle$ and $\langle \Delta E^2 \rangle$, according to equation (2). The collapse of the data obtained with different dynamics shows that the system stationary states are characterized by a *single* thermodynamic parameter. The agreement with the ensemble averages shows the success of Edwards' approach to describe the system macroscopic properties.

Figure 2 shows $\overline{E}$ (main frame) and $\overline{\Delta E}^2$ (inset) as functions of the tap amplitude, T_Γ (for several values of the tap duration, τ_0). Since sequences of taps with the same T_Γ and different τ_0 give different values of $\overline{E}$ and $\overline{\Delta E}^2$, it is apparent that T_Γ is not the right thermodynamic parameter. On the other hand, if the stationary states are indeed characterized by a *single* thermodynamic parameter the curves corresponding to different tap sequences (i.e. different T_Γ and τ_0) should collapse onto a single master function, when $\overline{\Delta E}^2$ is parametrically plotted as a function of $\overline{E}$. This is the case in the present model, where the data collapse is in fact found and shown in figure 3. This is a prediction that could be easily checked in real granular materials.

A technique to derive from raw data the thermodynamic parameter $\beta_{\rm fd}$ conjugated to E (apart from an integration constant, β_0) is through the usual *equilibrium* fluctuation–dissipation relation of equation (5). By integrating equations (5), (6) is obtained and $\beta_{\rm fd} - \beta_0$ can be expressed as a function of $\overline{E}$ or (for a fixed value of τ_0) as a function of $\beta_\Gamma = 1/T_\Gamma$: $\beta_{\rm fd} = \beta_{\rm fd}(\beta_\Gamma)$ (the constant β_0 can be determined as explained in [11]). Now, we use the

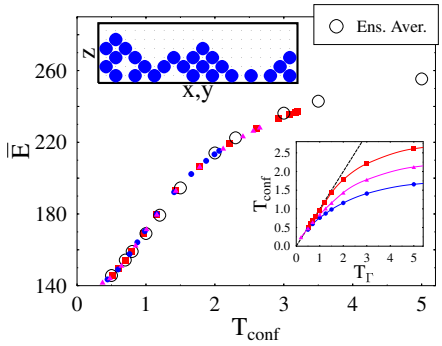

Figure 4. The time average $\overline{E}$ and the ensemble average over the distribution equation (2) $\langle E\rangle$, plotted respectively as a function of $T_{\rm fd}$ and $T_{\rm conf}$ (in units mga_0), in the 3D monodisperse hard-sphere system under gravity described in the text. Symbols are as in figure 3. Time averages over the tap dynamics and Edwards' ensemble averages coincide. Lower inset: the temperature $T_{\rm fd} \equiv T_{\rm conf}$ defined by equation (5) as a function of T_Γ (in units mga_0) for $\tau_0 = 500, 10, 5$ MCSs (from top to bottom). The straight line is the function $T_{\rm conf} = T_\Gamma$.

name $\beta_{\rm fd}$ for the thermodynamic parameter conjugated to E because we can conclude that $\beta_{\rm fd} = \beta_{\rm conf}$ only when the average over the tap dynamics and the ensemble average with equation (2) coincide. Thus, even though we have just shown that a 'thermodynamic', i.e., a statistical mechanics, description is indeed possible, we have still to show that specifically the distribution of equation (2) holds. This is accomplished in the next section and interesting novelties will be shown in section 5.

3.2. Ensemble averages

Summarizing, in section 3.1 we have found that the fluctuations of the energy in the stationary state depend only on the energy, E, and not on the past history. More generally, we found [11] that all the macroscopic quantities we observed depend only on the energy, E, or on its conjugate thermodynamic parameter, $\beta_{\rm fd}$, thus the stationary state can be genuinely considered a 'thermodynamic state'.

We show now that ensemble averages based on the theoretical distribution of equation (2) coincide with time averages over the tap dynamics. We compare, for instance, the time average of the energy, $\overline{E}(\beta_{\rm fd})$, recorded during the tap sequences, with the ensemble average, $\langle E\rangle(\beta_{\rm conf})$, over the distribution equation (2). With this aim we have independently calculated the ensemble average $\langle E\rangle$, as a function of $\beta_{\rm conf}$. Figure 4 (see also figure 3) shows a very good agreement between $\langle E\rangle(\beta_{\rm conf})$ and $\overline{E}(\beta_{\rm fd})$ (notice that there are no adjustable parameters). Such an agreement was found for all the observables we considered [11]. In figure 4 (inset) we also show the dependence of the configurational temperature $T_{\rm conf}$ on the parameters of the tap dynamics T_Γ and τ_0. Finally, we mention that we have also successfully tested Edwards' scenario in another model, the 'frustrated lattice gas' [33, 11], a system in the category of spin glasses.

3.3. The properties of the compaction 'tap' dynamics

The MC tap dynamics exhibits a rich structure in agreement with experimental findings [5, 7]. The system is prepared in an initial loose configuration and then tapped. Under tapping its density tends to increase as a function of the number of shakes, in a stretched exponential

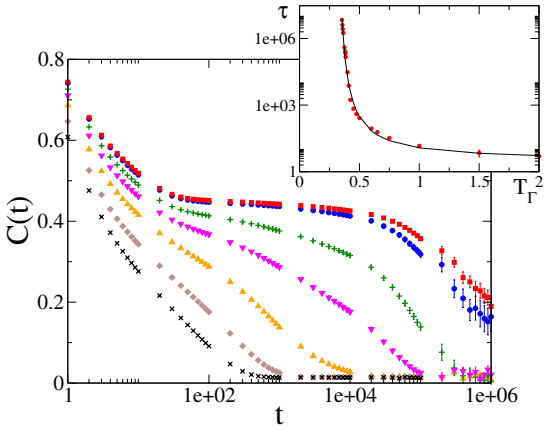

Figure 5. Main frame: the density correlation function in the TTI regime, $q(t) \equiv C(t)$, as a function of the number of taps, t, for several values of T_Γ, in a hard-sphere lattice model [37]. Inset: the characteristic relaxation time (in units of number of 'taps') as a function of the shaking amplitude T_Γ. A Vogel–Fulcher function, with a divergency at $T_K = 0.29$, fits the data (continuous line).

way at comparatively high T_Γ [11] and in a logarithmic way at small T_Γ [8]. This is in close correspondence with experimental findings from the Chicago [5] and Rennes [7] groups. At small amplitudes, 'irreversibility' [5, 8] and 'ageing' phenomena along with huge relaxation times diverging á la Arrhenius or Vogel and Fulcher [5–7] are found in these systems, similarly to glass formers in the freezing region.

It is interesting to consider density correlation functions such as $C(t, t_w) = B(t, t_w)/B(t_w, t_w)$, where $B(t, t_w) = \sum_i [\langle n_i(t + t_w) n_i(t_w)\rangle - \langle n_i(t + t_w)\rangle\langle n_i(t_w)\rangle]$. In the high T_Γ region, $C(t, t_w)$ has a time translation invariant (TTI) behaviour, i.e., $C(t, t_w) = C(t)$ (see the inset of figure 5). Asymptotically, $C(t)$ can be well fitted by stretched exponentials: $C(t) = C_0 \exp[-(t/\tau)^\beta]$ (here β is not the 'temperature', but just the stretching exponent of the exponential). The exponent β becomes significantly lower than unity at low amplitudes. The above fit defines the relaxation time $\tau(T_\Gamma)$ (see figure 5): the growth of τ by decreasing T_Γ is well approximated by an Arrhenius or Vogel–Tamman–Fulcher law (as earlier found in [8, 11]), resembling the slowing down of glass formers close to the glass transition, a result also recently experimentally reported in granular media [6, 7]: $\tau \simeq \tau_0 \exp[E_0/(T_\Gamma - T_\Gamma^K)]$. The divergence point, T_Γ^K (which in simulations is difficult to precisely locate and here consistent with zero), of τ is interpreted as the numerical location of the point of dynamical arrest of the system, where an 'ideal' transition to a glassy phase occurs. By quenching the system at low values of T_Γ, the TTI character of relaxation is lost and logarithmic ageing behaviours, as stated, are found. For slow quenches the hard-sphere model is able, anyway, to attain its crystal phase. The precise nature of the 'glassy' region, very difficult to numerically determine, is analytically investigated in the following sections.

3.4. Hard-sphere binary mixtures under gravity

In order to test the statistical mechanics approach in a more complicated system and to study segregation mechanisms, we also considered a hard-sphere binary system made of two species 1 (small) and 2 (large) with grain diameters a_0 and $\sqrt{2}a_0$, under gravity on a cubic lattice of spacing $a_0 = 1$. We set the units such that the two kinds of grain have masses $m_1 = 1$

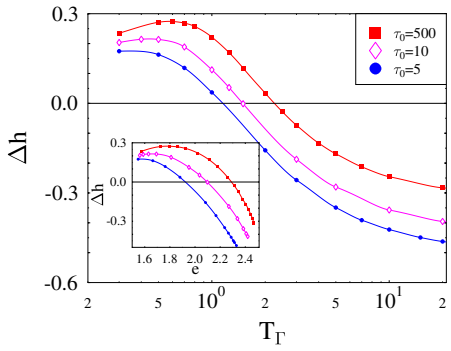

Figure 6. Main frame: the difference of the average heights of small and large grains, $\Delta h = h_1 - h_2$, measured at stationarity in the binary hard-sphere mixture under gravity, is plotted as a function of tap amplitude, T_Γ (in units mga_0). The three sets of points correspond to the shown tap durations, τ_0. At high T_Γ larger grains are found above the smaller, i.e., $\Delta h < 0$, as in the Brazil nut effect (BNE). Below a $T_\Gamma^*(\tau_0)$ the opposite is found (reverse Brazil nut effect, RBNE). Inset: the Δh data of the main frame are plotted as a function of the corresponding average energy, e. The three sets of data do not collapse, as before, onto a single master function.

and $m_2 = 2m_1$, and gravity acceleration is $g = 1$. The hard-core potential $\mathcal{H}_{\rm HC}$ is such that two large nearest-neighbour particles cannot overlap. This implies that only couples of small particles can be nearest neighbours on the lattice. The system overall Hamiltonian is

$$\mathcal{H} = \mathcal{H}_{\rm HC} + m_1 g H_1 + m_2 g H_2, \tag{8}$$

where $H_1 = \sum_i^{(1)} z_i$ and $H_2 = \sum_i^{(2)} z_i$, the height of site i is z_i and the two sums are over all particles of species 1 and 2, respectively. In the above units, the gravitational energies in a given configuration are thus $E_1 = H_1$ and $E_2 = 2H_2$.

As before, grains are confined in a box of linear size L with periodic boundary conditions in the horizontal directions and initially prepared in a random loose stable pack. Under the tap dynamics the system approaches a stationary state for each value of the tap parameters T_Γ and τ_0 used. In figure 6, we plot as a function of T_Γ (for several values of τ_0) the asymptotic value of the *vertical* segregation parameter, i.e., the difference of the average heights of the small and large grains at stationarity, $\Delta h(T_\Gamma, \tau_0) \equiv h_1 - h_2$. Here h_1 and h_2 are the averages of H_1/N_1 and H_2/N_2 over the tap dynamics at stationarity. Figure 6 shows that the Brazil nut effect (BNE, large grains above) is observed at high T_Γ, and the reverse BNE at smaller T_Γ. Before discussing segregation mechanisms, we want to check the statistical mechanics scenario described in the previous sections.

The results given in the main panel of figure 6 apparently show that T_Γ is not the right thermodynamic parameter, since sequences of taps with different τ_0 give different values for the system observables. However, if the stationary states corresponding to different tap dynamics (i.e., different T_Γ and τ_0) are indeed characterized by a single thermodynamic parameter, as in the monodisperse case above, the curves of figure 6 should collapse onto a universal master function when $\Delta h(T_\Gamma, \tau_0)$ is parametrically plotted as a function of an other macroscopic observable such as the average energy, $e(T_\Gamma, \tau_0) = (E_1 + E_2)/N$ (N is the total number of particles). This collapse of data is not observed here, as is apparent in the inset of figure 6. We found, instead [11], that two macroscopic quantities can be sufficient to characterize uniquely the stationary state of the system. These two quantities are, for instance, the energy e and the height difference Δh. Of course since $e = ah_1 + 2bh_2$ (where $a = N_1/N$ and $b = N_2/N$) and $\Delta h = h_1 - h_2$, we can also choose h_1 and h_2 to characterize the stationary state. Namely, we

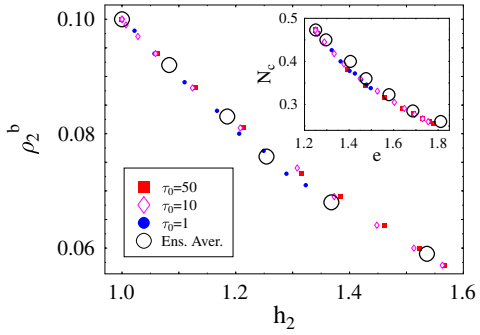

Figure 7. Main frame: the average density of large grains on the box bottom layer, ρ_2^b, measured at stationarity for different T_Γ and τ_0, scales almost on a single master function when plotted as a function of the large grain height, h_2. Upper inset: the average number of contacts between large grains per particle, N_c, obtained for different T_Γ and τ_0, scale on a single master function when plotted as a function of the system energy, e.

found that a generic macroscopic quantity A, averaged over the tap dynamics in the stationary state, is only dependent on h_1 and h_2, i.e., $A = A(h_1, h_2)$. We have checked that this is the case for several independent observables, such as the number of contacts between large particles, N_c, the density of small and large particles on the bottom layer, ρ_1^b and ρ_2^b, and others, as shown in figure 7. Therefore, we need both h_1 and h_2 to characterize unambiguously the state of the system; namely, all the observables assume the same values in a stationary state characterized by the same values of h_1 and h_2, independently of the previous history (i.e., in our case independently of the particular tapping parameters T_Γ and τ_0).

These findings imply that an extension of Edwards' original approach is required, where at least *two* thermodynamic parameters have to be included [11]. As before, this can be obtained by assuming that the microscopic distribution is given by the principle of maximum entropy with the constraint that the average gravitational energies of the two species $E_1 = \sum_r P_r E_{1r}$ and $E_2 = \sum_r P_r E_{2r}$ are independently fixed. This gives *two* Lagrange multipliers:

$$\beta_1 = \frac{\partial \ln \Omega(E_1, E_2)}{\partial E_1} \qquad \beta_2 = \frac{\partial \ln \Omega(E_1, E_2)}{\partial E_2} \tag{9}$$

where $\Omega(E_1, E_2)$ is the number of inherent states with E_1,E_2.

The hypothesis that the ensemble distribution at stationarity is the above can be tested as we have already previously shown. We have to check that the time average of any quantity, $A(h_1, h_2)$, as recorded during the tap sequences in a stationary state characterized by given values h_1 and h_2, coincides with the ensemble average, $\langle A \rangle(h_1, h_2)$, over the generalized version of distribution equation (2). With this aim, we have independently calculated the ensemble averages $\langle N_c \rangle$, $\langle \rho_2^b \rangle$, $\langle \rho_1^b \rangle$ for different values of β_1 and β_2; we have expressed parametrically $\langle N_c \rangle$, $\langle \rho_2^b \rangle$, $\langle \rho_1^b \rangle$, as a function of the average of h_1 and h_2, and compared them with the corresponding quantities, N_c, ρ_1^b and ρ_2^b, averaged over the tap dynamics. The two sets of data are plotted in figure 7 showing a good agreement (notice that there are no adjustable parameters). Figure 8 shows the two configurational temperatures $T_1 \equiv \beta_1^{-1}$ and $T_2 \equiv \beta_2^{-1}$ as a function of the tap amplitude, T_Γ.

Equation (9) shows that there are two distinct Lagrange multipliers, constraining independently the energy of the two species. A consequence of this fact is that in this approach, where the total energy is not constrained, the zero principle of thermodynamics does not necessarily hold. Indeed, only if the total energy $E_1 + E_2$ could be somehow kept constant, would one obtain by maximizing the entropy $\beta_1 = \beta_2$.

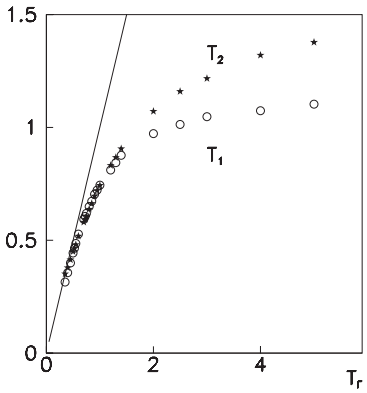

Figure 8. The configurational temperatures $T_1 \equiv \beta_1^{-1}$ (circles) and $T_2 \equiv \beta_2^{-1}$ (stars) as a function of the tap amplitude, T_Γ, for a tap duration $\tau_0 = 10$ MCS. The straight line is line $y = x$.

4. A mean field theory of the phase diagram of granular media

We have seen that even though granular media may form crystalline packings, in most cases they are found at rest in disordered configurations, characterized by 'fluid'-like distribution functions. Gently shaken granular media exhibit a strong form of 'jamming' [5–7], i.e., an exceedingly slow dynamics, which shows deep connections to 'freezing' phenomena observed in many thermal systems such as glass formers [8, 9].

An interesting result reported above is that in at least some schematic hard-sphere models, a statistical mechanics description of granular media appears to be well grounded. This allows us to evaluate the 'granular' partition function, Z, of equation (4) in order to derive the system phase diagram. This was accomplished for a monodisperse system, at a mean field level, in [34]. In an approximation á la Bethe–Peierls, we consider a system of hard spheres with a Hamiltonian given in equation (7) plus a chemical potential term to control the overall density. We adopt here a simple definition of 'mechanical stability': a grain is 'stable' if it has a grain underneath. The operator Π_r thus has a simple expression: $\Pi_r = \lim_{K\to\infty} \exp\{-K\mathcal{H}_{\rm Edw}\}$ where $\mathcal{H}_{\rm Edw} = \sum_i \delta_{n_i(z),1}\delta_{n_i(z-1),0}\delta_{n_i(z-2),0}$ (for clarity, we have shown the z dependence in $n_i(z)$).

By using the Bethe–Peierls approximation with the techniques of the 'cavity method' [3], the phase diagram is found [34]. At low $N_{\rm s}$ ($N_{\rm s}$ is the number of grains per unit surface) or high $T_{\rm conf}$ a fluid-like phase is found, characterized by a homogeneous replica symmetric (RS) solution, in which only one pure state exists and the local fields are the same for all the sites of the lattice (translational invariance). For a given $N_{\rm s}$, by lowering $T_{\rm conf}$ (see figures 9 and 10), a phase transition to a crystal phase (an RS solution with no space translation invariance) is found at $T_{\rm m}$. Notice that the fluid phase still exists below $T_{\rm m}$ as a metastable phase corresponding to a supercooled fluid found when crystallization is avoided.

Within the one-step replica symmetry breaking (1RSB) ansatz of the cavity method [3], a non-trivial solution appears for the first time at a given temperature $T_{\rm D}(N_{\rm s})$, signalling the existence of an exponentially high number of pure states. In mean field theory $T_{\rm D}$ is interpreted as the location of a purely dynamical transition as in mode-coupling theory, but in real systems it might just correspond to a crossover in the dynamics (see [24, 12, 35] and references therein). The 1RSB solution becomes stable at a lower point $T_{\rm K}$, where a thermodynamic transition from the supercooled fluid to a 1RSB glassy phase takes place (see figure 9) in a scenario á la Kauzmann with a vanishing complexity of pure states (which stays finite for $T_{\rm K} < T < T_{\rm D}$).

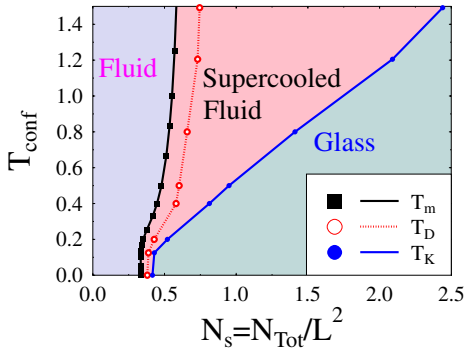

Figure 9. The system mean field phase diagram is plotted in the plane of its two control parameters ($T_{\rm conf}$, $N_{\rm s}$): $T_{\rm conf}$ is Edwards' 'configurational temperature' and $N_{\rm s}$ the average number of grains per unit surface in the box. At low $N_{\rm s}$ or high $T_{\rm conf}$, the system is found in a fluid phase. The fluid forms a crystal below a melting transition line $T_{\rm m}(N_{\rm s})$. When crystallization is avoided, the 'supercooled' (i.e., metastable) fluid has a thermodynamic phase transition, at a point $T_{\rm K}(N_{\rm s})$, to a replica symmetry breaking 'glassy' phase with the same structure found in mean field theory of glass formers. In between $T_{\rm m}(N_{\rm s})$ and $T_{\rm K}(N_{\rm s})$ a dynamical freezing point, $T_{\rm D}(N_{\rm s})$, is located, where the system characteristic timescales diverge.

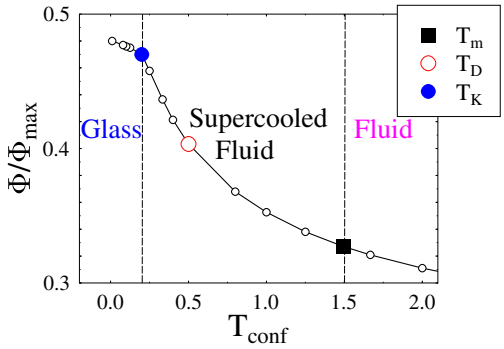

Figure 10. For a system with a given number of grains (i.e., a given $N_{\rm s}$), the overall number density, $\Phi \equiv N_{\rm s}/2\langle z\rangle$ ($\langle z\rangle$ is the average height), calculated in the mean field approximation, is plotted as a function of $T_{\rm conf}$; $\Phi(T_{\rm conf})$ has a shape very similar to the one observed in the 'reversible regime' of tap experiments and MC simulations of the cubic lattice model for $\Phi(T_\Gamma)$. The location of the glass transition, $T_{\rm K}$ (filled circle), corresponds to a cusp in the function $\Phi(T_{\rm conf})$. The passage from the fluid to supercooled fluid is $T_{\rm m}$ (filled square). The dynamical crossover point $T_{\rm D}$ is found around the flex of $\Phi(T_{\rm conf})$ and corresponds well to the position of a characteristic shaking amplitude Γ^* found in experiments and simulations where the 'irreversible' and 'reversible' regimes approximately meet.

The results of these calculations, summarized in the phase diagram of figure 9, are further illustrated in figure 10: in a system with a given number of grains (i.e., a given $N_{\rm s}$), the overall number density, Φ, is plotted as a function of $T_{\rm conf}$ (here by definition $\Phi \equiv N_{\rm s}/2\langle z\rangle$, where $\langle z\rangle$ is the average height). The shown curve, $\Phi(T_{\rm conf})$, is the equilibrium function calculated here. It has a shape very similar to the one observed in tap experiments [5, 7], or in MC simulations on the cubic lattice (see also [8]), where the density is plotted as a function of the shaking amplitude Γ (along the so called 'reversible branch'). In particular, a comparison of our mean field results with simulations of the 3D model of hard spheres under the tap dynamics shows a very good agreement.

Summarizing, in the present mean field scenario of a granular medium with N_s particles per surface, in general, at high T_{conf} (i.e. high shaking amplitudes) a fluid phase is located (see figure 9). By lowering T_{conf}, a phase transition to a crystal phase is found at T_m. However, when crystallization is avoided, the fluid phase still exists below T_m as a metastable phase corresponding to a supercooled fluid. At a lower point, T_D, an exponentially high number of new metastable states appears, interpreted, at a mean field level, as the location of a purely dynamical transition, which in a real system is thought to correspond just to a dynamical crossover. Finally, at an even lower point, T_K, the supercooled fluid has a genuinely thermodynamic discontinuous phase transition to the glassy state. The structure of the glass transition of the present model for granular media, obtained in the framework of Edwards' theory, is the same as found in the glass transition of the p-spin glass and in other mean field models for glass formers [24, 12].

4.1. A mean field theory of segregation

As an application of the statistical mechanics of powder mixtures just discussed, we now consider the intriguing phenomenon of segregation: in the presence of shaking a granular system is not randomized, but its components tend to separate [14]. An example is the so called 'Brazil nut' effect (BNE), where, under shaking, large particles rise to the top and small particles move to the bottom of the container. Interestingly, by changing grain sizes, mass ratio or shaking amplitudes a crossover towards a 'reverse Brazil nut' effect (RBNE) was more recently discovered [19] where small particles segregates to the top and large particles to the bottom (see figure 6). Several mechanisms have been proposed to explain these phenomena which, although of deep practical and conceptual relevance, are still largely unknown [14]. Geometric effects, such as 'percolation' [15] or 'reorganization' [16, 17], are known to be at work since, in a nutshell, small grains appear to filter beneath large ones. 'Dynamical' effects, such as convection [18] or inertia [20], were shown to play a role as well. Recent simulations and experiments have, however, outlined that segregation phenomena can involve 'global' mechanisms, such as 'condensation' [19] or, more generally, 'phase separation' [21]. We focus on these properties here.

We apply the mean field approximation of section 4 to the present binary mixture to give a statistical mechanics interpretation of segregation phenomena observed in the model of equation (8) and in the simulations of figure 6 (see also [36]). With the Bethe–Peierls methods the free energy, F, can be derived [36] along with the quantities of interest, such as the density profile of small and large grains, $\rho_1(z)$ and $\rho_2(z)$, and average heights $h_n = \langle z_n \rangle = \sum_z z\rho_n(z) / \sum_z \rho_n(z)$ (with $n = 1, 2$). The system parameters (for a given grain size ratio) are four: the two number densities per unit surface, N_1 and N_2, and the two configurational temperatures, or more precisely $m_1\beta_1$ and $m_2\beta_2$ (conjugated to gravitational energies). In the space of these parameters, the fluid phase corresponds to a solution of Bethe–Peierls equations where the density field in each layer is invariant under horizontal translations. A crystalline phase, characterized by the breakdown of the translational invariance (density fields are now different on neighbouring sites), is also found.

The typical system phase diagram in 3D is shown in figure 11 in the plane (N_1, N_2), i.e., densities per unit surface of species 1 and 2, in the case where $m_1\beta_1 > m_2\beta_2$. There are pure fluid and crystal phases, whose extension depends on $m_1\beta_1$ and $m_2\beta_2$ (they shrink as $m_1\beta_1$ and $m_2\beta_2$ increase). For clarity, figure 11 does not shows the metastable fluid phases of the system discussed in the previous section: a 'supercooled fluid', i.e., a fluid with a free energy higher than the crystal, and a glass. Since nucleation times can in practice be very long (and enhanced by a degree of polydispersity), crystallization can be avoided in granular media and the metastable fluid observed indeed.

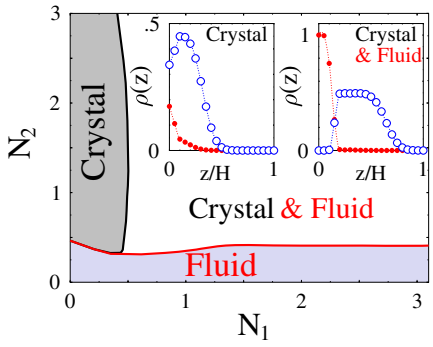

Figure 11. Mean field phase diagram of a 3D binary system under gravity, treated á la Edwards, in the density plane (N_1, N_2) for $m_1\beta_1 = 1$ and $m_2\beta_2 = 1/2$, where β_1 and m_1 (respectively β_2 and m_2) are the inverse configurational temperature and the mass of small grains (respectively large grains). A pure fluid and crystal phase are present. In the region marked 'Crystal & Fluid', a new state is found where the system, due to gravity, is vertically separated in a fluid and a crystal phase. Here the crystal, rich in large grains, is resting on a fluid bed, rich in small grains. This is a *phase separation induced segregation*, in a BNE configuration, visualized in the right inset: showing the density profiles of the two species, $\rho_1(z)$ and $\rho_2(z)$ (respectively filled and empty circles), as a function of the vertical coordinate z, at a typical point of the 'Crystal & Fluid' region with $N_1 = 3$, $N_2 = 4$. The reverse, i.e., RBNE with the fluid floating above the crystal, can be found when $m_1\beta_1 < m_2\beta_2$. For comparison in the left inset we show $\rho_1(z)$ and $\rho_2(z)$ at a point of the crystal phase with $N_1 = 0.3$, $N_2 = 4$: small grains are here interspersed with large ones even though, on average, slightly below. This illustrates that within a pure phase gravity and 'geometry' effects can also drive a different form of segregation, not associated with phase separation. For clarity, metastable phases are not shown in this phase diagram.

In the region marked 'Crystal & Fluid', a new absolute minimum of the free energy, F, is found, corresponding to a state where the system, due to gravity, is vertically separated in a fluid and a crystal phase. The presence of gravity breaks the 'up–down' symmetry and, for instance, in the 'Crystal & Fluid' region of figure 11 where $m_1\beta_1 > m_2\beta_2$, the crystal phase, rich in large grains, moves to the top and a clear cut BNE is found (as RBNE is observed in the opposite case, when $m_1\beta_1 < m_2\beta_2$). This is a *phase separation induced segregation*, where the two phases are divided by a sharp interface. The right inset of figure 11 plots the density profiles which, in this region, show a clear separation of the two coexisting phases.

Due to the symmetry breaking gravity field, in 3D no coarsening phenomena are usually associated with segregation. Coarsening is expected to appear when both the phase densities and the configurational temperatures get close, a phenomenon which could be tested by experiments or simulations.

Opposed to the above phase separation driven segregation, within the pure fluid and crystal phases one can also observe *mixing* or a simpler form of vertical segregation. This is shown, at a typical point of the crystal phase, by the species density profiles plotted in the left inset of figure 11: small grains are essentially mixed with large ones, even though, on average, slightly below. For a given ratio $m_1\beta_1/m_2\beta_2$, this form of segregation is generated by simple 'buoyancy' and 'geometrical' (also named 'percolation' [15]) mechanisms: for instance, in the left inset of figure 11 where $m_1\beta_1 > m_2\beta_2$, gravity tends to favour the rise of large grains as more mechanically stable states can be found with small grains at the bottom or, stated differently, small grains can more easily filter beneath larger ones to find stable states. Thus, in general, for a given grain size ratio, an interplay of mass densities and configurational temperatures difference drives the phases vertical positioning.

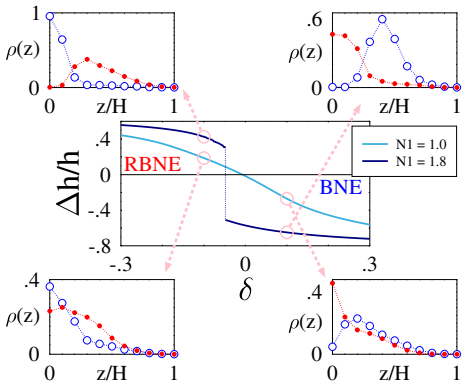

Figure 12. Main panel: the vertical segregation parameter $\Delta h/h$ is plotted as a function of $\delta = (m_2 - 2m_1)/(m_2 + 2m_1)$ in a binary granular system in its fluid phase in the case $\beta_1 = \beta_2 = 1$. For a given number of large grains, $N_2 = 1$, when $N_1 = 1$ by reducing δ the system smoothly crosses from BNE to RBNE, via a *mixing* region located around $\delta = 0$ where $\Delta h/h \sim 0$. When small grains are comparatively more abundant, $N_1 = 1.8$, the region where $\Delta h/h \sim 0$ disappears and around a critical value $\delta_c \neq 0$ the system has an abrupt transition from BNE to RBNE. Side panels: the density profiles $\rho(z)$ of the two species are plotted for $\delta = \pm 1$. Full (empty) circles correspond to small (large) grain density.

In order to illustrate further these effects, for simplicity, we consider now only the system fluid phase and we take the case $\beta_1 = \beta_2 = 1$. The segregation status of the system changes by changing the mass ratio parameter $\delta = (2m_1 - m_2)/(2m_1 + m_2)$: when $\delta \gg 0$ the BNE is expected to be found, as well as the RBNE when $\delta \ll 0$. This is indeed the case, as shown in the main panel of figure 12 which plots the usual vertical segregation parameter $\Delta h/h \equiv 2(h_1 - h_2)/(h_1 + h_2)$ as a function of δ (here h_1 and h_2 are the average heights of small and large grains). For a given number of large grains, $N_2 = 1$, in the case where there are comparatively few small grains, e.g., $N_1 = 1$, by reducing δ the system smoothly crosses from BNE to RBNE, via a *mixing* region located around $\delta = 0$ where $\Delta h/h \sim 0$ (see figure 12). When small grains are comparatively abundant, e.g., $N_1 = 1.8$, the scenario drastically changes for the enhanced role of depletion forces acting between large grains: the region where $\Delta h/h \sim 0$ disappears and around a critical value $\delta_c \neq 0$ the system has an abrupt transition from BNE to RBNE. The jump observed in $\Delta h/h$ is related to the crossing of a phase transition line present in the fluid phase (this is due to depletion forces between large grains and is, in fact, absent if grains have equal radii). In order to compare the properties of the system microscopic configurations, figure 12 also plots the density profiles $\rho(z)$ of the two species for $\delta = \pm 1$.

Summarizing, the present mean field statistical mechanics model of a granular binary mixture, here analytically treated á la Edwards, individuates two basic mechanisms underlying, in the absence of hydrodynamic modes, mixing and segregation phenomena corresponding to a variety of experimentally observed effects, ranging from BNE [14] and RBNE [19, 38] to coarsening [21]. In these non-thermal media there is a form of segregation which is related to thermodynamic-like mechanisms taking place in the system, i.e., phase transitions. A different kind of segregation phenomena exists, not associated with phase transitions, which is driven in pure phases by 'buoyancy' and 'geometric' effects.

5. Conclusions

An important open issue in the physics of granular media is the theoretical foundation and experimental test of statistical mechanics approaches and, in particular, the approach proposed

by Edwards and here briefly reviewed. In practice, the general validity of Edwards' scenario has just begun to be assessed and there are still many, crucial, open questions [2]. Within the schematic framework of simple hard-sphere models, we have shown that such an approach to dense granular media appears to be well grounded, and a first framework is emerging to understand their physics and their deep connections with thermal systems such as fluids and glass formers.

We have shown that the system stationary states are indeed independent of the sample history as in a 'thermodynamics' system, and can be described in terms of a distribution function characterized by a few control parameters (such as configurational temperatures). We then derived, by analytical calculations at a mean field level, the phase diagram of these systems. In particular, we discovered that 'jamming' corresponds to a phase transition from a 'fluid' to a 'glassy' phase, observed when crystallization is avoided. Interestingly, the nature of such a 'glassy' phase turns out to be the same as found in mean field models for glass formers. In the same framework, we have also discussed segregation patterns observed in hard-sphere binary systems, where Edwards' original approach must be extended. Here, the presence of fluid–crystal phase transitions in the system drives segregation as a form of phase separation. Within a given phase, gravity can also induce a kind of 'vertical' segregation, not associated with phase transitions.

As a first reference picture is emerging in the physics of dense granular media, a deeper test of these theories and their consequences, the experimental determination of the described phase diagram and segregation features and the connections to hydrodynamics effects are among relevant open research directions ahead in this field.

Acknowledgments

Work supported by MIUR-PRIN 2002/FIRB 2002, CRdC-AMRA, INFM-PCI and EU MRTN-CT-2003-504712.

References

[1] Edwards S F and Oakeshott R B S 1989 *Physica* A **157** 1080
Mehta A and Edwards S F 1989 *Physica* A **157** 1091
Edwards S F 1991 *Disorder in Condensed Matter Physics* Oxford Science Publishers, p 148
Mehta A (ed) 1994 *Granular Matter: an Interdisciplinary Approach* (New York: Springer)
[2] Coniglio A, Fierro A, Herrmann H J and Nicodemi M (ed) 2004 *Unifying Concepts in Granular Media and Glasses* (Amsterdam: Elsevier)
[3] Mézard M and Parisi G 2001 *Eur. Phys. J.* B **20** 217
Mézard M and Parisi G 2003 *J. Stat. Phys.* **111** 1
[4] Jaeger H M, Nagel S R and Behringer R P 1996 *Rev. Mod. Phys.* **68** 1259
[5] Knight J B, Fandrich C G, Lau C N, Jaeger H M and Nagel S R 1995 *Phys. Rev.* E **51** 3957
Nowak E R, Knight J B, Ben-Naim E, Jaeger H M and Nagel S R 1998 *Phys. Rev.* E **57** 1971
Nowak E R, Knight J B, Povinelli M, Jaeger H M and Nagel S R 1997 *Powder Technol.* **94** 79
[6] D'Anna G and Gremaud G 2001 *Nature* **413** 407
[7] Philippe P and Bideau D 2002 *Europhys. Lett.* **60** 677
[8] Nicodemi M, Coniglio A and Herrmann H J 1997 *Phys. Rev.* E **55** 3962
Nicodemi M, Coniglio A and Herrmann H J 1997 *J. Phys. A: Math. Gen.* **30** L379
[9] Liu A J and Nagel S R 1998 *Nature* **396** 21
[10] O'Hern C S, Langer S A, Liu A J and Nagel S R 2001 *Phys. Rev. Lett.* **86** 111
O'Hern C S, Silbert L E, Liu A J and Nagel S R 2003 *Phys. Rev.* E **68** 011306
[11] Fierro A, Nicodemi M and Coniglio A 2002 *Europhys. Lett.* **59** 642
Fierro A, Nicodemi M and Coniglio A 2002 *Phys. Rev.* E **66** 061301
Fierro A, Nicodemi M and Coniglio A 2002 *Europhys. Lett.* **60** 684

[12] Biroli G and Mézard M 2002 *Phys. Rev. Lett.* **88** 025501
[13] Makse H A and Kurchan J 2002 *Nature* **415** 614
[14] Ottino J M and Khakhar D V 2000 *Annu. Rev. Fluid Mech.* **32** 55
Bridgewater J 1994 *Chem. Eng. Sci.* **50** 4081
[15] Rosato T, Prinze F, Standburg K J and Swendsen R 1987 *Phys. Rev. Lett.* **58** 1038
[16] Bridgewater J 1976 *Powder Technol.* **15** 215
Williams J C 1976 *Powder Technol.* **15** 245
[17] Duran J, Rajchenbach J and Clement E 1993 *Phys. Rev. Lett.* **70** 2431
[18] Knight J, Jaeger H and Nagel S 1993 *Phys. Rev. Lett.* **70** 3728
[19] Hong D C, Quinn P V and Luding S 2001 *Phys. Rev. Lett.* **86** 3423
Both J A and Hong D C 2002 *Phys. Rev. Lett.* **88** 124301
[20] Shinbrot T and Muzzio F 1988 *Phys. Rev. Lett.* **81** 4365
[21] Hill K M and Kakalios J 1994 *Phys. Rev.* E **49** R3610
Reis P M and Mullin T 2002 *Phys. Rev. Lett.* **89** 244301
Aumaitre S, Schnautz T, Kruelle C A and Rehberg I 2003 *Phys. Rev. Lett.* **90** 114302
[22] Cugliandolo L F, Kurchan J and Peliti L 1997 *Phys. Rev.* E **55** 3898–914
[23] Cugliandolo L F and Kurchan J 1993 *Phys. Rev. Lett.* **71** 173–6
[24] Cugliandolo L and Kurchan J 1993 *Phys. Rev. Lett.* **71** 173
Kurchan J 2001 *Jamming and Rheology: Constrained Dynamics on Microscopic and Macroscopic Scales* ed A J Liu and S R Nagel (London: Taylor and Francis)
[25] Nicodemi M 1999 *Phys. Rev. Lett.* **82** 3734
[26] Barrat A *et al* 2000 *Phys. Rev. Lett.* **85** 5034
[27] Coniglio A and Nicodemi M 2001 *Physica* A **296** 451
[28] Brey J J, Prados A and Sánchez-Rey B 2000 *Physica* A **275** 310
[29] Dean D S and Lefèvre A 2001 *Phys. Rev. Lett.* **86** 5639
[30] Tarjus G and Viot P 2004 *Phys. Rev.* E **69** 011307
[31] Berg J, Franz S and Sellitto M 2002 *Eur. Phys. J.* B **26** 349
[32] Berg J and Mehta A 2001 *Europhys. Lett.* **56** 784
[33] Coniglio A, de Candia A, Fierro A and Nicodemi M 1999 *J. Phys.: Condens. Matter* **11** A167
[34] Tarzia M, de Candia A, Fierro A, Nicodemi M and Coniglio A 2004 *Europhys. Lett.* **66** 531
[35] Toninelli C, Biroli G and Fisher D S 2003 *Preprint* cond-mat/0306746
[36] Tarzia M, Fierro A, Nicodemi M and Coniglio A 2004 *Phys. Rev. Lett.* **93** 198002
[37] Tarzia M, Fierro A, Nicodemi M and Coniglio A 2005 in preparation
[38] Breu A P J, Ensner H-M, Kruelle C A and Rehberg I 2003 *Phys. Rev. Lett.* **90** 014302